ISBN: 978-3-95450-184-7 doi:10.18429/JACoW-IPAC2018-MOPML002

STATUS OF THE JLEIC ION COLLIDER RING DESIGN

G.H. Wei†, V.S. Morozov, F. Lin, Y. Zhang
Jefferson Lab, Newport News, VA 23606, USA
Y. Cai, Y.M. Nosochkov, SLAC, Menlo Park, CA 94025, USA

Abstract

This paper presents an update on the design of the ion collider ring of the Jefferson Lab Electron Ion Collider (JLEIC). Based on the existed lattice and optics with chromaticity compensation, tune optimization was studied. We investigate the dependence of the dynamic aperture on the betatron tune in order to search for a large dynamic aperture. Dynamic analysis with on-momentum and off-momentum are included. Meanwhile, the several correction scenarios of coherent orbits caused by detector solenoid and the crossing angle of 50 mrad are also presented.

LATTICE AND BEAM OPTICS OF THE JLEIC ION COLLIDER RING

The JLEIC ion collider ring accelerates protons from 8 to up to 100 GeV/c or ions in the equivalent momentum range and is designed to provide luminosity above 10^{33} cm^{-2}s^{-1} [1, 2]. The overall collision lattice of the ion collider ring is shown in Fig. 1. The ring consists of two 261.7 ° arcs connected by two straight sections intersecting at an 81.7° angle. The total circumference of the ion collider ring is 2153.89 m.

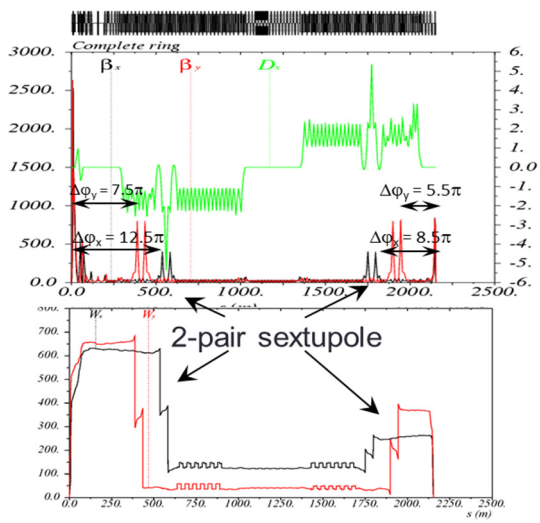

Figure 1: Linear optics (upper plot with phase advances of chromatic sextupoles) and chromaticity compensation (lower plot with w function) of the JLEIC ion collider ring starting from IP.

The JLEIC ion collider ring has 292 main magnets including 133 dipoles, 205 quadrupoles, and 54 sextupoles. In the interaction region (IR), there are 1 dipoles and 6 final focus quadrupoles whose beta functions are about very large and asymmetric. The large beta at Final Focus Quadrupole causes a strong chromatic kick to the β-function in δ=Δp/p [3]. Non-interleaved −I sextupole pairs on each side of IP are used to compensate these chromatic kicks. The chromatic amplitude function (equation (1), w function in MADX) is compensated to 0 at IP. The remaining linear chromaticity is cancelled by using 48 two-family sextupoles, where ξx and ξy are set to +1 for the whole lattice.

$$w = \sqrt{a^2 + b^2}\,, \text{ where } b = \frac{1}{\beta}\frac{\partial \beta}{\partial p_t},\ a = \frac{\partial \alpha}{\partial p_t} - \alpha b \quad (1)$$

TUNE OPTIMIZATION

The dynamic aperture gives a description of the nonlinear effects arising from sextupoles to correct for the chromaticity and the field imperfections of the magnets. It is necessary to estimate how large the dynamic aperture in a machine is. And the tune in a lattice and optics should be optimized to have a good dynamic aperture.

Dynamic Aperture with Tune Scanning

In the lattice of the ion collider ring, there is a FODO section for tune adjustment surrounded by two matching sections. We scan the tune by adjusting tune in this section. And the tune scanning range is (24.0, 23.0) to (24.5, 23.5). Here the tune scanning step is 0.01 for both Qx and Qy, so that totally there are about 2500 working points. And we choose the interaction point (IP) as the dynamic aperture study position.

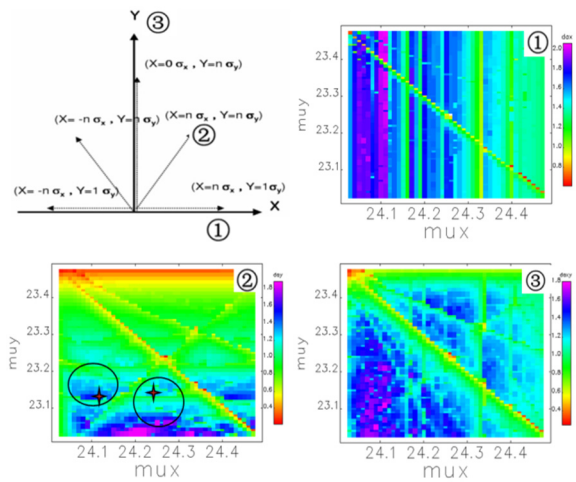

Figure 2: Survey of the dynamic aperture in the X-Y plane. (upper-left: survey method; upper-right: dynamic aperture survey result along horizontal direction; lower-left: dynamic aperture survey result along 45° direction; lower-right: dynamic aperture survey result along vertical direction;)

† gwei@jlab.org

ISBN: 978-3-95450-184-7 doi:10.18429/JACoW-IPAC2018-MOPML002

And on each of those 2500 points, we calculate the dynamic aperture along three directions. As shown in upper-left figure of Fig. 2, we selected x direction with a vertical offset of 1 sigma of vertical beam size, a 45° direction, and vertical direction. The dynamic aperture results in these three directions are shown in 3 figures of Fig. 2 with direction marks.

The dynamic aperture with x direction scanning shows big influence from ν_x-ν_y, $2\nu_x$, and $3\nu_x$. Result of the 45° direction survey shows resonance lines of ν_x+ν_y, ν_x-$2\nu_y$, and $2\nu_y$, etc. Result of the verticle direction survey shows resonance lines of $6\nu_x$, etc. From these 3 results, we found two areas with good dynamic apertures, centred by tune (24.22, 23.16) and tune (24.1, 23.14).

On-momentum Analysis

After the dynamic aperture study with tune scanning, we continue to study the nonlinear effects with on-momentum beam mainly on the selected two working points. Here we use frequency map to study the dynamic aperture and tune footprint as shown in Fig. 3.

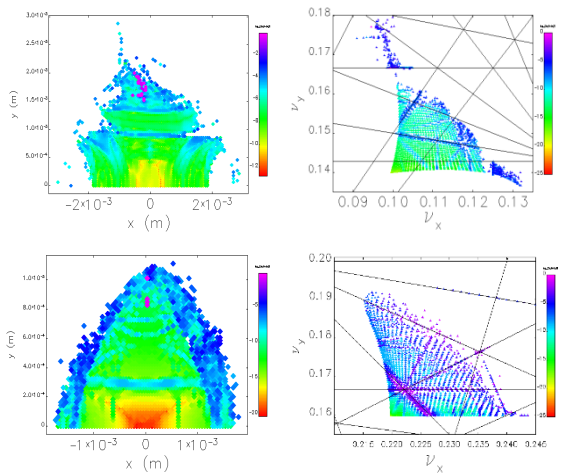

Figure 3: Frequency map of dynamic aperture and tune footprint for tune (24.22, 23.16) (two figures upper, left one for dynamic aperture and right one for tune footprint) and tune (24.1, 23.14) (two figures lower, left one for dynamic aperture and right one for tune footprint). The resonance lines are plotted up to seventh order.

The FMA diffusion rate is plotted as a colour weighted value. We can find a bigger dynamic aperture with the tune (24.1, 23.14), but a more stable core area of dynamic aperture with the tune (24.22, 23.16). In the tune footprint, several resonance lines can be identified for these two tunes, like ν_x+$6\nu_y$, $7\nu_x$, and $3\nu_x$-$2\nu_y$ for the tune (24.1, 23.14), and $3\nu_x$, $3\nu_x$+$2\nu_y$, and $2\nu_x$-$5\nu_y$ for the tune (24. 22, 23.16).

Off-momentum Analysis

The momentum dependence of tune and β∗ are corrected for the off-momentum analysis. We adjust the phase advances between IP and the chromatic sextupoles to have a momentum-dependence tune as flat as possible. And tune offset at 0.5 % of momentum offset is also controlled in the optimization. Here β∗ , tune, and dynamic aperture results with off-momentum of ± 0.5 % are shown in Fig. 4.

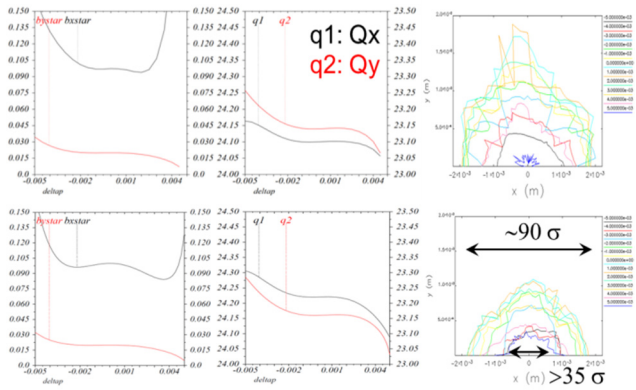

Figure 4: β∗ (left), tune (middle), and dynamic aperture (right) versus δp for the tune (24.22, 23.16) (upper 3 figures) and the tune (24.1, 23.14) (lower 3 figures)

Here from the β∗ plots versus δp for the two tune, we find the β∗ with 0.5 % of off-momentum beam has very large value for the tune (24.1, 23.14). And we can also see the tune (24.1, 23.14) has obvious asymmetric dynamic apertures between positive momentum offset and negative momentum offset, especially at ± 0.5 %. Meanwhile the tune (24.22, 23.16) has dynamic apertures of larger than 35 sigma of beam size at ± 0.5 %, and about 90 sigma of beam size with on-momentum beam. Thus currently, we choose the tune (24.22, 23.16) for further study. And the tune (24.1, 23.14) has larger dynamic aperture at ± 0.3 %, which makes it a good option also.

COMPENSATION SCENARIOS OF DETECTOR SOLENOID EFFCTS

The detector solenoid causes coherent orbit distortion. The orbit correction of the beam orbit uses two dipole correctors on each side of the IP to make not only orbit but also orbit slope to be 0 at IP and coherent orbit controlled between the two FFQ triplets in IR [4]. But in one hand, the IR area is so tight especially the downstream section of the IP, we should make correctors comfortably aligning in the area; in another hand, the nuclear physics and magnet requirement want weak fields of these correctors. Thus we studied other options for detector solenoid compensation.

Compensation Scenarios of Detector Solenoid Effects at Collision Energy

In original design, as shown in the upper-left figure in Fig. 5, there are 4 correctors with lengths of 0.2 meter. The third corrector will have a big strength of 1.6 T. For the new scenarios, the first one, as shown in right-left figure in Fig. 5, has 0.6 meter correctors instead of 0.2 meter correctors as shown in the upper-right figure in Fig. 5. This scenario reduces the strengths of correctors. The largest one is the first upstream corrector with 0.7 T.

ISBN: 978-3-95450-184-7 doi:10.18429/JACoW-IPAC2018-MOPML002

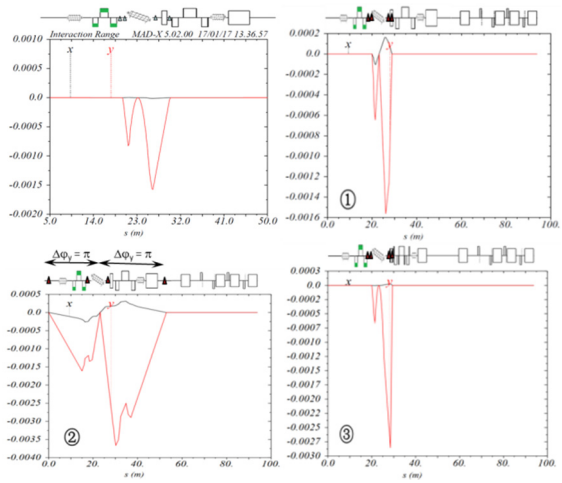

Figure 5: Scenarios of coherent orbit correction in the IR of the JLEIC ion ring (upper-left: original design with 0.2 meter long correctors; upper-right: a long corrector scenario, lower-left: a pi phase advance corrector scenario, lower-right: a scenario of 1st dipole nested with a corrector)

The third scenario, as shown in the lower-right figure, has a corrector nested in the first dipole. This one saves spaces but have a large orbit of 3 mm. Another scenario, as shown in the lower-left figure, the two correctors each side of the IP have a phase advance of pi. This scenario saves the space in IR, and strengths of correctors are lower. But it brings offsets of closed orbit in IR triplets.

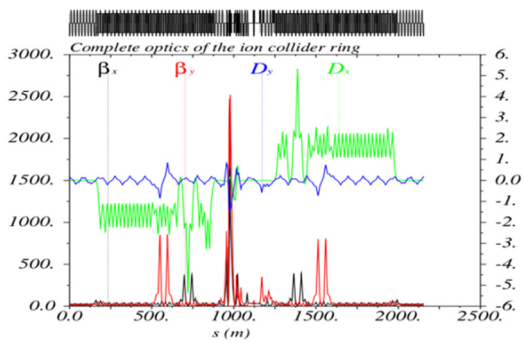

Figure 6: Beta and dispersion functions around the ion collider ring in the pi phase-advance corrector scenario.

And the scenario with a pi phase-advance correctors gives vertical dispersion effect, as shown in Fig. 6, which is needed to be carefully considered. This vertical dispersion influences on the IBS Growth Rates, as shown in table 1. It reduces the longitudinal IBS growth time and increase the horizontal IBS growth time. We can use skew quads at locations where horizontal dispersion is not zero to compensate the vertical dispersion. However, skew quads also create coupling effects which is also needed to consider in the further study. Meanwhile it is good to have a longer transverse IBS growth time which complex the picture.

Table 1: Magnets in the JLEIC Ion Collider Ring

	Detector Solenoid off	Scenarios with correctors between the two triplets	the π phase-advance correctors scenario
τ_l [h]	5.824	5.809	3.770
τ_x [h]	0.444	0.444	0.731
τ_y [h]	22.538	21.958	9.443

Compensation Scenarios of Detector Solenoid Effects at Injection Energy

Detector solenoid can't easily ramp as normal magnets. Here we think a design with detector solenoid of 3 T at injection energy. Because we don't need to have orbit zero at IP, we can adjust the whole coherent orbit in IR, as shown in Fig. 7. The coherent orbit is adjusted to 7 mm rather than a big offset of 20 mm at injection.

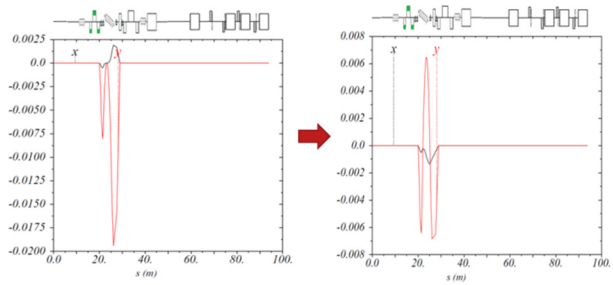

Figure 7: Coherent orbit correction in the IR of the JLEIC ion ring at injection energy

ACKNOWLEDGMENT

This manuscript has been authored by Jefferson Science Associates, LLC under U.S. DOE Contracts No. DE-AC05-06OR23177 and DE-AC02-06CH11357. Work supported also by the U.S. DOE Contract DE-AC02-76SF00515. The United States Government retains a non-exclusive, paid-up, irrevocable, world-wide license to publish or reproduce the published form.

REFERENCES

[1] S. Abeyratne *et al.*, arXiv:1504.07961 [physics.acc-ph].
[2] V.S. Morozov *et al.*, in *Proc. IPAC'14*, Dresden, Germany, Jun. 2014, paper MOPRO005, pp. 71-74.
[3] Y. Nosochkov *et al.*, in *Proc. IPAC'15*, Richmond, USA, May 2015, paper TUPWI032, pp. 2311-2314.
[4] G.H. Wei *et al.*, in *Proc. IPAC'16*, Busan, Korea, May 2016, p. 2454, doi:10.18429/JACoW-IPAC2016-WEPMW015.